Synthesis of Fluorene Based Alternating Copolymers using Direct Arylation Polymerization

Mohd Sani Sarjadi[iD], Yap Leong Khen, Xin Lin Wong, Zuhair Jamain[iD] and Md Lutfor Rahman[*,iD]

Faculty of Science & Natural Resources, Universiti Malaysia Sabah, 88400 Kota Kinabalu, Sabah, Malaysia

*Corresponding author: Tel/Fax: +6 088 3205661; E-mail: lutfor73@gmail.com

Many researches have been done to obtain a low band gap and high Polymeric solar cell (PSCs) polymer either by creating new polymer or revising reported polymers from previous studies. In present work, two new copolymers were synthesized through direct arylation polymerization to produce poly(9,9-didodecylfluorene-*alt*-benzo[*c*][1,2,5]thiadiazole (**P1**) and poly(9,9-didodecylfluorene-alt-thieno[3,2-*b*]thiophene) (**P2**). The **P1** and **P2** are donor-acceptor copolymers. **P1** and **P2** were compared to investigate its suitability to be applied in PSCs. The polymers obtained were characterized using FT-IR, NMR and UV-Vis spectroscopy. **P1** shows two adsorption bands at λ_{max1} = 243 nm and λ_{max2} = 320 nm, whereas **P2** also shows two adsorption bands at λ_{max1} = 243 nm and λ_{max2} = 427 nm. The optical band gap was calculated, **P1** enabled band gap of 3.88 eV while **P2** showed band gap of 2.91 eV. This work could be provided an insight to design and synthesize more efficient fluorene-based copolymers as active layer of PSCs in due course.

Keywords: Polymeric solar cell, Fluorine, Copolymer, Arylation.

INTRODUCTION

Global energy demand has been growing drastically since the inception of industrial revolution and expected to exceed 25 terawatts (TW) by 2035 [1-3]. Nowadays, various type of renewable energy resources, *e.g.* biofuel, hydro- or wind power, geothermal and solar energy, are highly preferable than the non-renewable energy sources, *e.g.* petroleum, coal, natural gas, *etc*. Due to renewable energy abundance and more environmental friendly compared to non-renewable energy sources.

Solar energy is one of the most attracting energy sources as the earth is constantly received sunlight throughout the life [4]. Solar energy is non-polluting, universal, decentralized and freely available energy sources. In order to harvest the sunlight, solar collector or photovoltaic cell is needed. Solar collector converts incident solar radiation into heat while photovoltaic cell converts incident solar radiation into electricity.

Basically, photovoltaic can be classified into either organic or inorganic while organic photovoltaics (OPVs) could be grouped into either quantum dots, dye-sensitized or polymeric solar cells (PSCs) [5]. Organic photovoltaics are attractive to replace expansive inorganic photovoltaic. Polymeric solar cells (PSCs) have light weight, flexible, semi-transparency, many

raw materials, low materials and manufacturing cost [6]. Power conversion efficiency (PCE) value is used to express the effectiveness of a photovoltaic to generate useful working electrical energy output from the light energy harvested from the sunlight. Lately, PCE achieved by the PSCs have been surpassed 12-16% [7], yet it is still far lag behind as compared with its inorganic counterparts, which have already break through 25% [8]. Hence, there are still rooms to catch up for the organic photovoltaics.

Besides, photovoltaic researches are focused on the production of low band-gapped conjugated polymers as the electron donating material of PSCs. Several modifications and invention have been performed by researchers to produce the novel conjugated polymers with desired properties [9,10]. Amongst these conjugated polymers, the well-known poly[*N*-9'-hepdecanyl-2,7-carbazole-alt-5,5-(4,7-di-2-thienyl-2′,1′,3′-benzothiadiazole] (PCDTBT) has widely been studied and successfully tested in real-world conditions [11].

Fluorene is one of the widely used as electron donating moiety of PSCs. Fluorene unit are commonly used to design a donor-acceptor conjugated polymers, (D-A) due to its highly conjugated structure, rigidity, high hole mobility, good chemical and thermal stability [12]. It is composed of a biphenyl connected by a methylene bridge and does not consist of any

heteroatoms *e.g.* S, N and O. The two protons at the 9-position are acidic, which can easily generated fluorenyl anion readily participates in nucleophilic substitution reactions with alkyl- or aryl-based electrophiles [12]. Various fluorene derivatives have been synthesized and commercially available in market.

Fluorene is a weak electron donating moiety when its 9-position was substituted by alkyl able to increase its electron donating ability and improve solubility [12]. An acceptor or π-linker are normally coupled with fluorene to tune its energy gap and energy level through intramolecular charge transfer effect by extending linear π-conjugation through molecular backbone of D-A copolymer [13]. Forming of D-A copolymer help to generate a strong push-pull driving force further enhance electron delocalization [13]. Fluorene based D-A copolymer formed should be able to achieve several requirements to provide promising PCE. The requirements are excellent solubility, strong and board light absorption, high charge mobility and well aligned energy level of highest occupied molecular orbital (HOMO) and lowest unoccupied molecular orbital (LUMO) [14].

Cheng *et al.* [15] has successfully synthesized an alternating copolymer consist of 9,9-dihexylfluorene and theino-[3,2-*b*]thiophene unit through Suzuki coupling. This copolymer unit with a maximum adsorption of 430 nm in chloroform was reported. Photovoltaic cell with the configuration of ITO/PEDOT/copolymer:PCBM (1:1, w/w)/Ca/Ag were fabricated and obtained a PCE of about 2 %. An alternating 9,9-dioctyl-fluorene and 2,1,3-benzothiadiazole copolymer unit was also synthesized through Suzuki coupling. The copolymer showed reduced in LUMO level able to improve electron mobility. The polymer as electron acceptor to blend with triarylamine based polyflourene as electron donor to form a photovoltaic cell by fabricating the polymer blend electron acceptor/electron donor (1:1, w/w) as the active layer and deposited between ITO and Al electrodes. A low external quantum efficiency (EQE) value of 4% at excitation energy of 3.2 eV was reported. A ternary blend solar cell of P3HT:PCBM/copolymer (1.0:0.6:1.4, wt %) with a PCE of 1.94 % was obtained [15].

In this study, two new D-A copolymers were designed and synthesized through direct arylation polymerization. 9,9-Didodecyl-2,7-dibromofluorene (**MA**), where 9-position of fluorene was substituted by two symmetrical branch alkyl chains as electron donating moiety and able improve solubility of polymer formed. This copolymer is an existing fluorene derivative but only receive little attraction from researchers and with limited publications and has potential to be applied in PSCs and electronic devices such as light-emitted diode (LEDs), opto-electronic devices and field-effect transistors (FEDs). Other copolymers *viz.* 2,1,3-benzothiadiazole (**MB**) and thieno-[3,2-*b*]thiophene (**MC**) acted as electron accepting moiety and widely used as acceptor or π-linker in PSCs. When copolymer **MA** coupled with another copolymer **MB** to form poly(9,9-didodecylfluorene-alt-benzo[*c*][1,2,5]thiadiazole) (**P1**) and **MA** coupled with **MC**, it forms poly(9,9-didodecylfluorene-alt-thieno[3,2-*b*]thiophene) (**P2**). Then, **P1** and **P2** were used to investigate the effect of this acceptor or π-linker toward the optical band gap of **MA** and suitability to apply as active layer in polymeric solar cells (PSCs).

EXPERIMENTAL

Monomers *viz.* 9,9-didodecyl-2,7-dibromofluorene (**MA**), 2,1,3-benzothiadiazole (**MB**) and thieno[3,2-*b*]thiophene (**MC**) were used as received without further purification and purchased from Sigma-Aldrich (Germany). The solvents were purchased from Nacalai Tesque (Japan), Merck (Germany), Fluka (China) and BDH (Japan). The reactions for the polymers synthesis were carried out under nitrogen atmosphere.

Synthesis of poly(9,9-didodecylfluorene-*alt*-benzo[*c*]-[1,2,5]thiadiazole) (P1): 9,9-Didodecyl-2,7-dibromofluorene (260 mg) and 2,1,3-benzothiadiazole (53.7 mg), palladium(II) acetate (10 mg), pivalic acid (12.1 mg) and anhydrous K_2CO_3 (81.7 mg) were stirred in anhydrous dimethylacetamide (3 mL) under inert nitrogen atmosphere. The mixture was degassed and heated to 110 °C for 72 h. After 72 h, the mixture was cooled to room temperature and thiophene (1 mL) was added. Then, the mixture was degassed and heated again to 110 °C for 3 h. After 3 h, the mixture was cooled to room temperature and cold methanol (30 mL) was added to the mixture. The solution mixture was stored in refrigerator overnight to enhance precipitation. The solution was filtered by using membrane filter and the collected solid was dissolved by using chloroform (20 mL). The dissolved solid in chloroform was then added dropwise into cold methanol (30 mL). The solution was cooled in refrigerator overnight and the solid was collected by filtration through a membrane filter. Again, dissolve and precipitation process repeated another two times. After repeated twice, the solid collected was air dried in fume hood (**Scheme-I**). Yield: 140 mg (56%), colour: green, phase: solid.
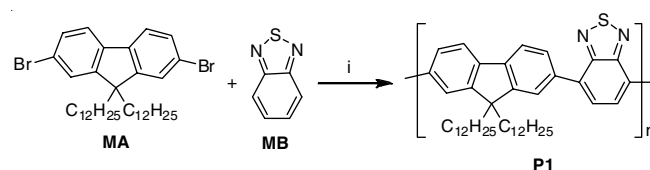
Scheme-I: Reaction scheme for synthesis of poly(9,9-didodecylfluorene-*alt*-benzo[*c*][1,2,5]thiadiazole) (**P1**). (i) Pd(OAc)₂, K₂CO₃, pivalic acid, dimethylacetamide, 100 °C, 72 h

Synthesis of poly(9,9-didodecylfluorene-*alt*-thieno[3,2-b]thiophene) (P2): The **P2** copolymer was synthesized in the similar procedure as mentioned above using thieno[3,2-*b*]-thiophene (55.3 mg) instead of 2,1,3-benzothiadiazole (**Scheme-II**). Yield: 144 mg (57.1%), colour: orange-red, phase: gel.
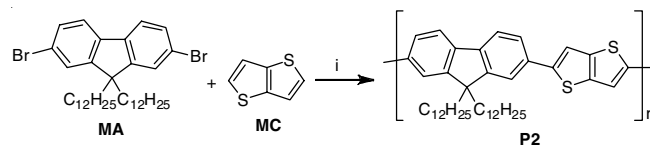
Scheme-II: Reaction scheme for synthesis of poly(9,9-didodecylfluorene-alt-thieno[3,2-*b*]thiophene) (**P2**). (i) Pd(OAc)₂, K₂CO₃, pivalic acid, dimethylacetamide, 100 °C, 72 h

Characterization: The characterization of **P1** and **P2** copolymers were carried out using the spectroscopic method. The colour and phase of **P1** and **P2** were observed. Thin layer

chromatography (TLC) was tested by using TLC silica gel 60 F_{254} (width = 3.7 cm and length = 7.0 cm) as stationary phase and hexane:ethyl acetate (5:1) as mobile phase. The spot of monomers and polymer were observed by using Cole Palmer Ultraviolent lamp box with 3 types of wavelength 254, 302 and 365 nm. Fourier transform-infrared spectrometer (FT-IR) adsorption spectra were recorded on the Agilent Cary 630 FT-IR spectrometer using a Germanium ATR attachment for sample analysis. FT-IR analysis was recorded in the range of 400 to 4000 cm^{-1} without using potassium bromide (KBr) pellets. UV-visible adsorption spectra were measured by Agilent Cary 60 Double Beam UV-Vis spectrometer. Measurement were conducted under wavelength of 200 to 600 nm, data interval of 1 nm, average time of 1.0 s and spectral bandwidth of 2 nm. The absorbance of polymers was measured in solution of chloroform at ambient temperature using rectangle quartz curvettes (light path length = 10 mm). Nuclear magnetic resonance (NMR) spectra were recorded on Bruker 500 MHz NMR spectrometers with deuterated chloroform (CDCl$_3$) solution.

RESULTS AND DISCUSSION

Since synthesized copolymers **P1** and **P2** produced from the direct arylation polymerization reaction under same synthetic procedure and conditions, therefore the yield of **P1** and **P2** are nearly same and acceptable. Before purification of polymer, TLC was used to ensure the reaction was completed with minimum amount of unreacted monomers and existent of polymer. Spots of **MA**, **MB** and **P1** on TLC were viewed under different wavelengths by using UV. The **P1** were formed but unreacted reactants still can be obseoved in the end reaction. As shown in Fig. 1, from the left point 1 is **MA**, point 2 is **MB** and point 3 is **P1** under different wavelengths. It was observed that **P1** was present in point 3 depicted as a small dot on middle of TLC while above the spot was the unreacted monomers.
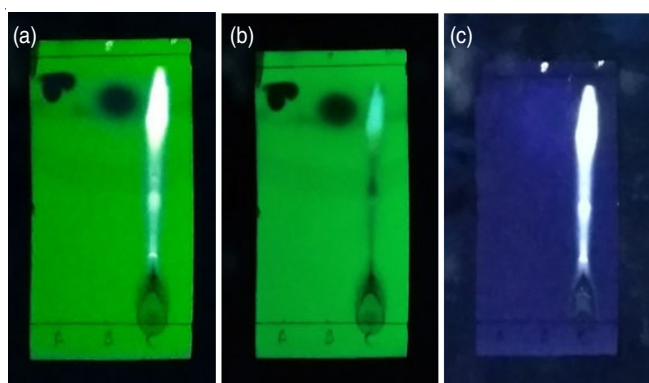

Fig. 1.   TLC of **MA**, **MB** and **P1** in UV-box under different wavelength of lights. (a) 254 nm; (b) 302 nm and (c) 365 nm

In Fig. 2 starting from the left, point 1 is **MA**, point 2 is **MB** and point 3 is **P2** under different wavelengths. It was observed that **P2** was present in point 3 as a small dot on middle of TLC while above the spot was the unreacted monomers. From the TLC of **P1** and **P2**, it can be observed that both of the spot for polymers were brighter under 254 nm and 365 nm wavelength.
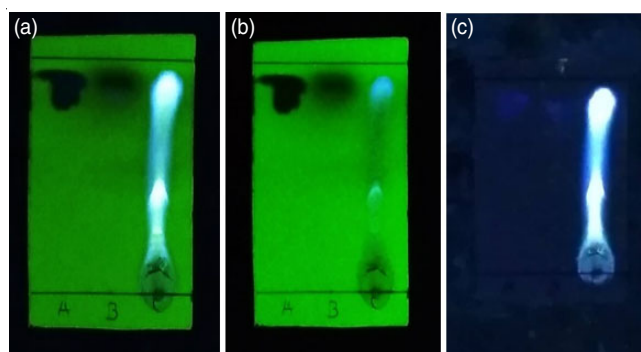

Fig. 2.   TLC of **MA**, **MB** and **P2** in UV-box under different wavelength of lights. (a) 254 nm; (b) 302 nm and (c) 365 nm

FT-IR analysis: The FTIR data of the synthesized **P1** and **P2** are summarized in Table-1. The strong peaks at 2850 and 2919 cm^{-1} are assigned to alkyl stretching of methylene groups. The characteristic overtone at 2078 cm^{-1} caused by C-H bending of aromatic ring was observed in the spectrum. The characteristic peak at 1454 cm^{-1} is due to bending of methylene –CH$_2$ groups. The peaks can be observed at 1571 cm^{-1} was assigned to the aromatic –C=C– stretching. The C-Br bending was observed at 805 cm^{-1}. Meanwhile, a medium peak for –CH$_3$ methyl group at 1350 cm^{-1} was not observed due to overlapping of methylene groups. A board peak at 1017 cm^{-1} was assigned for the combination band from constituent monomers, where **MA** exhibits peaks at 1057 and 1129 cm^{-1}, while **MB** exihibits peaks at 1127 cm^{-1}. A medium sharp C=N peak was not clearly appeared at range of 1690-1640 cm^{-1} due to the stronger effect of aromatic –C=C– stretching in **P1** causing overlapping of the peaks.

Polymer	Peak (cm^{-1})	Functional group
		TABLE-1
		KEY FTIR BANDS (cm^{-1}) OF **P1** AND **P2**
P1	805	C-Br bending
	1454	Bending of –CH$_2$ methylene groups
	1571	Aromatic –C=C- stretching
	2078	C-H bending of aromatic ring
	2850 and 2919	Alkyl stretching of methylene groups
P2	805	C-Br bending
	1362	Bending of methyl –CH$_3$
	1454	Bending of methylene –CH$_2$ groups
	1506	Aromatic –C=C- stretching
	1603 and 1688	Cyclic C=C stretching
	2108	C-H bending of aromatic ring
	2848 and 2917	Alkyl stretching of methylene groups

Similar to **P1**, copolymer **P2** showed the strong peaks at 2848 and 2917 cm^{-1} for alkyl stretching of methylene groups. The characteristic overtone at 2108 cm^{-1} was caused by the C-H bending of aromatic ring also seen in the spectrum. The characteristic peak at 1454 cm^{-1} was assigned for the bending of -CH$_2$ while the peak at 1362 cm^{-1} was assigned to bending of -CH$_3$. Moreover, the medium peaks at 1633 and 1688 cm^{-1} were assigned to the cyclic C=C stretching. The peaks for aromatic -C=C- stretching can be observed at 1506 cm^{-1}. Three sharp peaks at 911, 1183 and 1338 cm^{-1} observed in **MC**, was appe-

ared in **P2** at 999, 1174 and 1362 cm^{-1}. The peak at 805 cm^{-1} was assigned for C-Br bending for the **MA** core system.

NMR analysis: ^{1}H NMR studies of **P1** was conducted at 25 ºC in deuterated chloroform to confirm its structure. ^{1}H NMR spectrum of **P1** is shown in Fig. 3. The **P1** has unsymmetrical structure with 58 hydrogens. From ^{1}H NMR spectrum, aromatic region of proton for fluorene hydrogen showed multiplet signal in the range of δ 7.24-7.52 ppm and benzothiadiazole hydrogen showed multiplet signal in the range of δ 7.53-7.96 ppm. The benzothiadiazole hydrogen labeled as **e** and **d** was assigned at the most deshielded aromatic protons due to the electronegative of nitrogen and sulphur atom in the molecules. The peak assigned as **d** will the most deshielded hydrogen as it further from the electron donating fluorene. Besides, proton signals for alkyl chain of fluorene were observed in upfield region. The signal **f** experience more deshielded compared to other alkyl chain protons as it is nearest to electron withdrawing benzothiadiazole. The proton signal of **f** was appeared as multiplet signal at the range of δ 1.88-1.98 ppm. The signal for **g** to **o** assigned at δ 1.13-1.21 ppm was appeared as a triplet since its proton experienced the similar chemical environment. A triplet proton signal at δ 0.77-0.79 ppm at the most up field region was assigned to **p** and **q** as both hydrogen was furthest from the electron withdrawing benzothiadiazole.
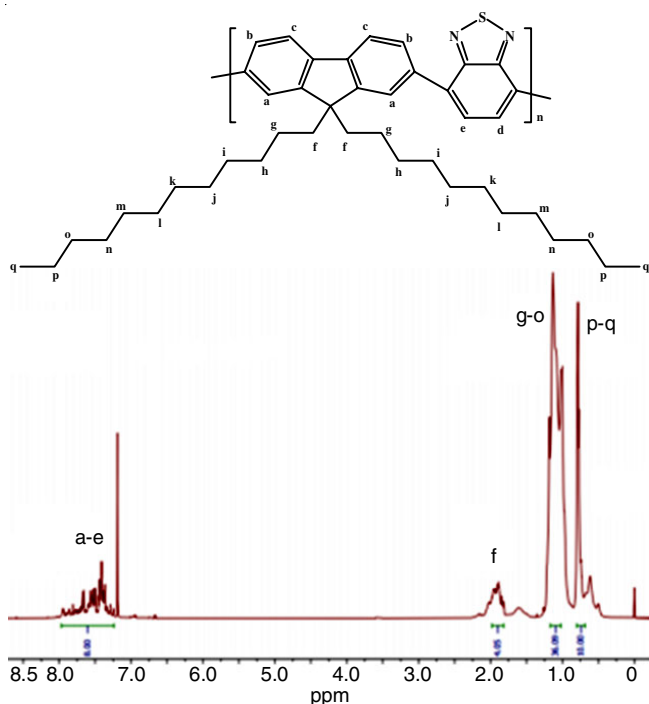

Fig. 4. ^{13}C NMR (151 MHz, CDCl$_3$) spectrum for **P1**

Fig. 3. ^{1}H NMR (600 MHz, CDCl$_3$) spectrum for **P1**

The ^{13}C NMR spectrum of copolymer **P1** has a total of 17 carbon signals (Fig. 4). The aromatic carbon signals were observed at δ 120.02 ppm was assigned to C9 and C11, at δ 121.04 and 121.09 ppm, respectively. The signal at 121.41 ppm was assigned to C8, C14 and C16, at δ 126.23 ppm assigned to C2, C15 and C17, while at δ 130.01 ppm assigned to C4 & C5, respectively. Besides, more deshielded aromatic carbon signals observed at δ 139.34 ppm, which assigned to C3 and C6, at δ

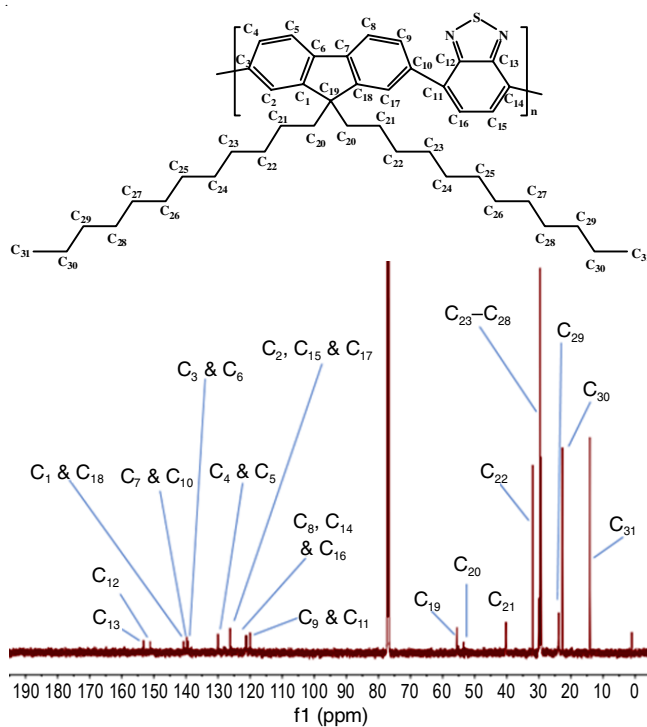139.77 ppm was assigned to C7 and C10, while at δ 140.76 ppm was assigned to C1 and C18. On the other hand, most deshielded aromatic carbon signal at δ 151.15 and 153.25 ppm were assigned to C12 and C13 due to the electro-negativity effect of nitrogen and sulphur atom, respectively. The C13 was more deshielded than C12 due to the location of C13, which further away from the electron donating fluorene group. The C19 was assigned for quaternary carbon at δ 55.54 ppm, while C20 which attached with C19 was assigned at δ 53.43 ppm.

The carbon signal at δ 40.25 and 31.92 ppm was assigned to C21 and C22, respectively. While, C23 to C28 was assigned at the range of δ 29.24-31.92 ppm due to the overlapping of carbon signals. The two-alkyl chain showed almost same pulling force from the electron withdrawing benzothiadiazole, which causes overlapping of carbon signals. The carbon signals at δ 14.13, 22.69 and 23.79 ppm were assigned to C31, C30 and C29, respectively. These three carbon signals appeared at upfield due to it is furthest from the electron withdrawing benzothiadiazole. The ^{1}H NMR and ^{13}C NMR spectra of **P2** also revealed the same pattern of **P1**. Both spectra only showed slightly different due to the chemical environment, bond angles and electronegativity of the **MB** and **MC** core system [16].

UV-visible analysis: The UV-Vis absorption spectra of **MA**, **MB** and **MC** were measured in chloroform. The **MA**, **MB** and **MC** exhibited absorption band at λ$_{max}$ = 283, 307 and 271 nm, respectively (Fig. 5). By measuring the absorption spectra of constituent monomers able to compare the improvement in absorption wavelength of light with the copolymers formed. The UV-Vis absorption spectra of the **P1** and **P2** were measured in chloroform. Fig. 6 showed that **P1** has two absorption band at λ$_{max1}$ = 243 nm and λ$_{max2}$ = 320 nm while **P2** has two absorption band at λ$_{max1}$ = 242 nm and λ$_{max2}$ = 427 nm.
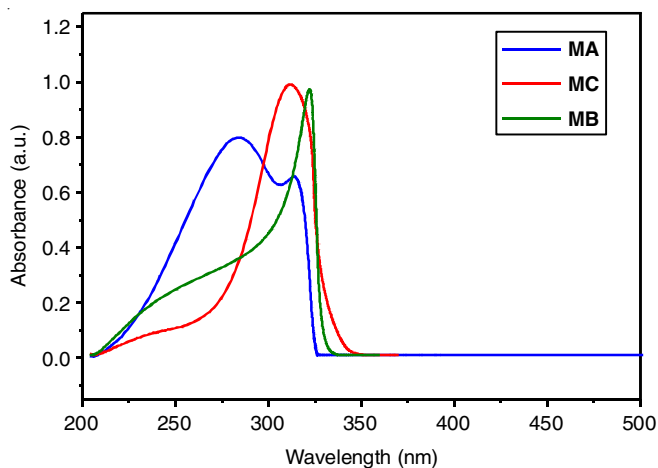
Fig. 5. Normalized UV-Vis spectra of **MA**, **MB** and **MC** in chloroform
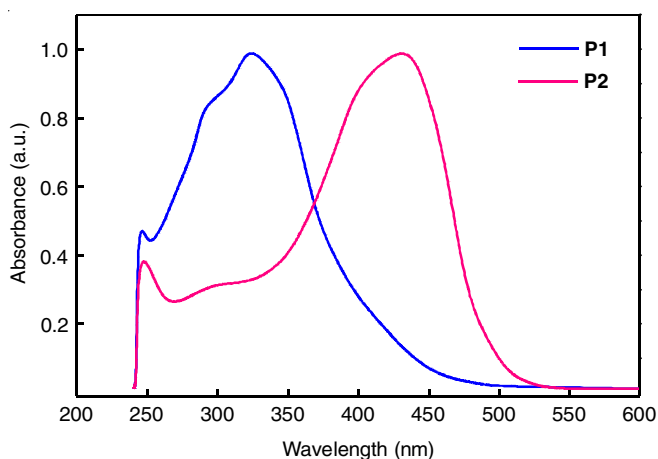
Fig. 6. Normalized UV-Vis spectra of **P1** and **P2** in chloroform

The optical band gaps of **MA**, **MB**, **MC**, **P1** and **P2** were calculated from onset of absorption spectra in chloroform and are summarized in Table-2. The calculated optical band gap value of **MA**, **MB**, **MC** was calculated was found to be E_g = 4.38, 4.04 eV and 4.58 eV, respectively. Among the monomers, **MB** has the smallest optical band gap. To efficiently conversion of solar energy to electrical energy by PSCs, small band gap and ability to harvest long wavelength of photon are necessary [16]. Solar radiation reach earth consists of ultraviolet, visible and infrared light with different wavelength. Since **MA**, **MB** and **MC** only able to absorb light at ultraviolent region which are not effective to be applied in PSCs. By forming **P1** and **P2** able to improve the absorption range and lower the optical band gap. The absorption spectrum of **P1** have absorption band at λ_{max} located in the ultraviolent region while **P2** have absorption band at λ_{max} located in the ultraviolent region and visible light region. The optical band gap for **P1** was calculated has a value of E_g = 3.88 eV while **P2** has a value of E_g = 2.91 eV. **P2** showed better potential in application of PSCs since it has lower optical band gap compared to **P1**. **P2** also able to harvest longer wavelength of light compare to **P1** as λ_{max} of **P2** is higher than **P1**. A lower optical band gap polymer able to has a more promising PCE. It can be noticed that one of the λ_{max1} is the same for **P1** and **P2** (λ_{max} = 243 nm), as **MA** was present in **P1** and **P2**.

TABLE-2
SUMMARY OF THE BAND GAP FOR **MA**, **MB**, **MC**, **P1** AND **P2**

Sample	λ_{max} (nm)	E_g (eV)
MA	283	4.38
MB	307	4.04
MC	271	4.58
P1	320	3.88
P2	427	2.91

Generally forming of D-A copolymer will provide lower optical band gap compared to constituent monomers. In order to tune the optical band gap for D-A copolymer, energy level of the highest occupied molecular orbital (HOMO) of donor unit and lowest unoccupied molecular orbital (LUMO) of acceptor unit is needed to be well aligned [15,16]. In **P2**, the donor-acceptor HOMO and LUMO energy level was well align caused it has increased in λ_{max} when compared to **MA**. Besides, the optical band gap of **P2** also decrease compared to **MA**. However in **P1**, the donor-acceptor HOMO and LUMO energy level was not well aligned. Although it also increased in λ_{max} and obtain lower optical band gap but the value was not much different from **MA**.

Conclusion

Two coplymers, *viz.* poly(9,9-didodecylfluorene-*alt*-benzo-[c][1,2,5]thiadiazole) (**P1**) and poly(9,9-didodecylfluorene-*alt*-thieno[3,2-*b*]thiophene) (**P2**) composed of alternating fluorene based copolymer unit were successfully synthesized by direct arylation polymerization. **P1** composed of alternating fluorene as donor unit and 2,1,3-benzothiadiazole as acceptor unit while **P2** composed of alternating fluorene as donor unit and thieno-[3,2-*b*]thiophene as acceptor unit. The structure of **P1** and **P2** were confirmed by IR, ^{1}H & ^{13}C NMR spectral data. The λ_{max} and range of adsorption of **P1** and **P2** were identified and optical band gap were also calculated. **P2** has a high potential as organic material applied in polymeric solar cell compared to **P1**, since **P2** has a better adsorption range and lower optical band gap. Coupling of 9,9-didodecyl-2,7-dibromofluorene (**MA**) with an acceptor or π-linker able to obtain better properties fluorene based polymers.

CONFLICT OF INTEREST

The authors declare that there is no conflict of interests regarding the publication of this article.

REFERENCES

1. L. Etgar, *Materials*, **6**, 445 (2013);
   https://doi.org/10.3390/ma6020445
2. Q. An, F. Zhang, J. Zhang, W. Tang, Z. Deng and B. Hu, *Energy Environ. Sci.*, **9**, 281 (2016);
   https://doi.org/10.1039/C5EE02641E
3. X.L. Wong, M.L. Rahman and M.S. Sarjadi, *Int. J. Electrochem. Sci.*, **12**, 6315 (2017);
   https://doi.org/10.20964/2017.07.76

4. S.E. Tan, F.H. Anuar, M.S. Sarkar, M.L. Rahman and M.S. Sarjadi, *ChemistrySelect*, **4**, 936 (2019);
https://doi.org/10.1002/slct.201801259

5. S. Richard, *Sustainable Energy*, **2**, 85 (2014);
https://doi.org/10.7569/JSEE.2014.629506

6. N. Kannan and D. Vakeesan, *Renew. Sustain. Energy Rev.*, **62**, 1092 (2016);
https://doi.org/10.1016/j.rser.2016.05.022

7. L. Dou, W.H. Chang, J. Gao, C.C. Chen, J. You and Y. Yang, *Adv. Mater.*, **25**, 825 (2013);
https://doi.org/10.1002/adma.201203827

8. J. Kuwabara, Y. Nohara, S.J. Choi, Y. Fujinami, W. Lu, K. Yoshimura, J. Oguma, K. Suenobu and T. Kanbara, *Polym. Chem.*, **4**, 947 (2013);
https://doi.org/10.1039/C2PY20917A

9. C. Lupangu and R.C. Bansal, *Renew. Sustain. Energy Rev.*, **73**, 950 (2017);
https://doi.org/10.1016/j.rser.2017.02.003

10. J.J.R. Arias, L. Crociani, I.T. Soares, I.C. Mota, B.P.S. Santos, R. Valaski and M.D.F.V. Marques, *React. Funct. Polym.*, **144**, 104355 (2019);
https://doi.org/10.1016/j.reactfunctpolym.2019.104355

11. Y. Xu, G. Hai, H. Xu, H. Zhang, Z. Zuo, Q. Zhang, R. Xia, C. Sun, J. Castro-Smirnov, A. Sousaraei, S. Casado, M.R. Osorio, D. Granados, I. Rodriguez and J. Cabanillas-Gonzalez, *Adv. Opt. Mater.*, **6**, 1800263 (2018);
https://doi.org/10.1002/adom.201800263

12. S. Suman, A. Bagui, A. Garg, B. Tyagi, V. Gupta and S.P. Singh, *Chem. Commun.*, **54**, 4001 (2018);
https://doi.org/10.1039/C7CC08440D

13. X. Song, Y. Zhang, Y. Li, F. Li, X. Bao, D. Ding, M. Sun and R. Yang, *Macromolecules*, **50**, 6880 (2017);
https://doi.org/10.1021/acs.macromol.7b00998

14. S. Suman, A. Bagui, R. Datt, V. Gupta and S.P. Singh, *Chem. Commun.*, **53**, 12790 (2017);
https://doi.org/10.1039/C7CC08237A

15. Y.J. Cheng, S.H. Yang and C.S. Hsu, *Chem. Rev.*, **109**, 5868 (2009);
https://doi.org/10.1021/cr900182s

16. M.S. Sarjadi and A. Iraqi, *Polym. Polymer Compos.*, **24**, 703 (2016);
https://doi.org/10.1177/096739111602400905